Cerebral Cortex December 2008;18:2748–2761
doi:10.1093/cercor/bhn033
Advance Access publication March 20, 2008

Transient Neuronal Correlations Underlying Goal Selection and Maintenance in Prefrontal Cortex

Satoshi Tsujimoto, Aldo Genovesio and Steven P. Wise

Laboratory of Systems Neuroscience, National Institute of Mental Health, Building 49, Room B1EE17, 49 Convent Drive, MSC 4401, Bethesda, MD 20892-4401, USA

We reported previously that as monkeys used abstract response strategies to choose spatial goals, 1 population of prefrontal cortex neurons encoded future goals (F cells), whereas a largely separate population encoded previous goals (P cells). Here, to better understand the mechanisms of goal selection and maintenance, we studied correlated activity among pairs of these neurons. Among the 3 possible types of pairs, F-F and F-P pairs often exhibited significant correlations when and after monkeys selected future goals but P–P pairs rarely did. These correlations were stronger when monkeys shifted from a previous goal than when they stayed with that goal. In addition, members of F–F pairs usually preferred the same goal and thus shared both prospective coding and spatial tuning properties. In contrast, cells composing F–P pairs usually had different spatial preferences and thus shared neither coding nor spatial tuning properties. On the assumption that the neurons composing a pair send convergent outputs to target neurons, their correlated activity could enhance their efficacy in context-dependent goal selection, goal maintenance, and the transformation of goal choices into action.

Keywords: attentional selection, behavioral neurophysiology, cell assemblies, frontal lobe, working memory

Introduction

Ever since Hebb (1949), it has been assumed that neural representations arise among assemblies of interacting cells. Cell assemblies have several important properties, including the ability to be dynamically constructed and deconstructed, as reflected in event-related changes in correlated activity (Nicolelis et al. 1997; Sakurai 1999). Although such correlations have been documented in several brain regions (Vaadia et al. 1995; Riehle et al. 1997; Engel et al. 2001; Bair et al. 2001; Katz et al. 2002; Jackson et al. 2003; Sakurai and Takahashi 2006), little is known about their contribution to high-level cognitive processes, such as selecting goals by abstract response strategies.

A hallmark function of the prefrontal cortex is to monitor, select, and maintain behavioral goals (Owen et al. 1996; Rowe et al. 2000; Rowe and Passingham 2001; Saito et al. 2005; Mushiake et al. 2006), but its mechanisms remain poorly understood. Several neurophysiological studies have assessed the role of the prefrontal cortex in the short-term memory of places, objects, and stimulus features, with both retrospective (Fuster and Alexander 1971; Funahashi et al. 1989; Miller et al. 1996; Rainer et al. 1998; Kim and Shadlen 1999; Romo et al. 1999; Tsujimoto and Sawaguchi 2005; Amemori and Sawaguchi 2006; Zaksas and Pasternak 2006) and prospective (Hasegawa et al. 1998; Rainer et al. 1999; Fukushima et al. 2004; Saito et al. 2005) coding being well documented. Likewise, both neuroimaging (Owen et al. 1996; Cohen et al. 1997; Owen et al. 1999; Postle et al. 1999; Rowe et al. 2000; Rowe and Passingham 2001; Fletcher and Henson 2001) and neurocomputational (Rougier et al. 2005; O'Reilly 2006; O'Reilly and Frank 2006) studies have implicated the prefrontal cortex in updating and manipulating information stored in short-term memory. In accord with these findings, we showed previously that when monkeys used previous spatial goals to select future ones, prefrontal cortex neurons collectively encoded both previous and future goals. Individual neurons, however, typically encoded either previous or future goals but not both (Genovesio et al. 2006).

The present study explored the mechanisms for goal-directed behavior in the abstract strategy task of Genovesio et al. (2005). To do so, we computed joint perievent time histograms (JPETHs) (Aertsen et al. 1989; Sillito et al. 1994; Vaadia et al. 1995; Brown et al. 2004), which are 2-dimensional histograms that display the correlated activity of 2 neurons relative to a behavioral event. The main diagonal of a JPETH, called the *coincidence histogram*, displays how frequently both neurons discharge within the time bin chosen for analysis. One idea about such transient correlations is that they result from recurrent, excitatory loops within a neural network, which can sustain persistent neuronal activity (Amit et al. 1994; Amit and Brunel 1997; Camperi and Wang 1998; Wang 2001; Constantinidis and Wang 2004). Alternatively, Vaadia et al. (1995) pointed out that such correlations could occur with sparse, if any, synaptic connections between cells and that a temporal correlation per se could have potential functional significance regardless of its cause. Accordingly, we examined these discharge correlations in a population of prefrontal cortex neurons that encoded either a previous goal or a future goal, chosen by monkeys according to specific behavioral strategies.

Materials and Methods

Subjects and Behavioral Task

Two adult, male rhesus monkeys (*Macaca mulatta*), 8.8 and 7.7 kg, were studied. The monkeys were restrained comfortably in a primate chair, with their heads stabilized facing a video screen 32 cm away. All procedures accorded with the requirements and recommendations of the *Guide for the Care and Use of Laboratory Animals* (1996, ISBN 0-309-05377-3), and all aspects of the research were approved by the appropriate Animal Care and Use Committee. The monkeys were motivated to perform the task with fluid control.

Figure 1*A* illustrates the task, 1st used by Genovesio et al. (2005). After a 2.5-s intertrial interval, a white circle (0.7° visual angle), called the *fixation spot*, appeared at the center of the video screen. Once the monkeys fixated this location, 3 2.2° squares appeared 14° from the fixation point. These squares were potential goals for a saccadic eye

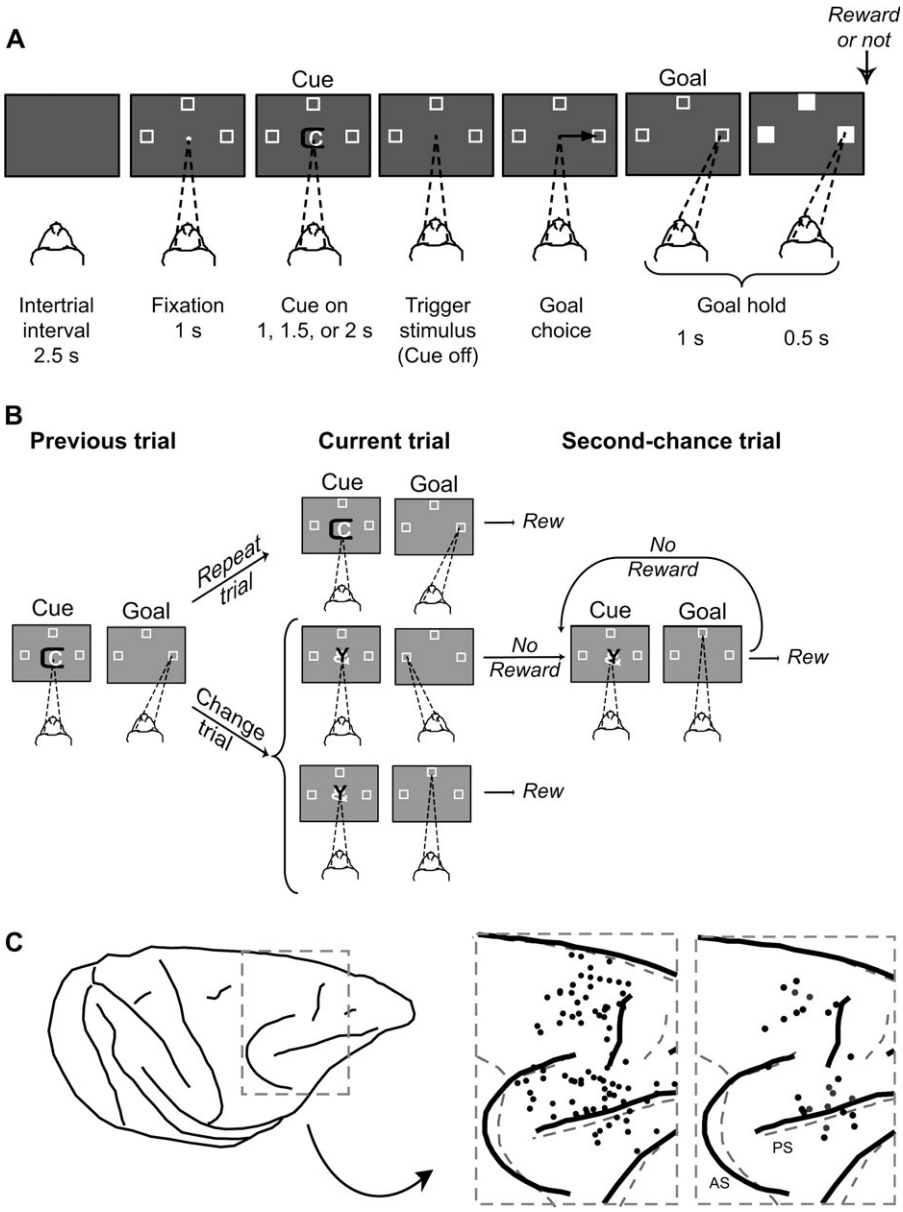

Figure 1. Task design and recording locations. (**A**) Sequence of task events. Each gray rectangle represents the video screen. On the screen, a central white circle (fixation point) and 3 white squares (potential goals) appeared on each trial. The dashed lines show the monkey's gaze angle and fixation target. Next, the cue appeared, and its offset triggered a saccade (black arrow)—to the right goal, in this example. (**B**) Previous, current, and 2nd-chance trials. On each current trial, a visual cue was selected pseudorandomly from a set of 3 cues. If the cue had repeated from the previous trial (called repeat trials), then staying with the most recent goal (the right one, in this example) produced a reward on the current trial. If the cue had changed (change trials), then the previous goal should be rejected in favor of 1 of the 2 alternatives, but the choice of only 1 of these (the top one, in this example) produced a reward. Rewarded choices ended a trial, but unrewarded choices led to 2nd-chance trials until a reward was obtained. Rew, reward. (**C**) Penetration sites: composite from both monkeys, relative to sulcal landmarks. Left to right: Drawing of 1 monkey's brain with the inset marked by a dashed gray box. The 1st inset (from left to right) shows the penetration sites for the overall population (black circles). The dashed gray sulcal lines show the alignment with the 2nd monkey. The 2nd inset shows the penetration sites for the pairs studied here (monkey 1, black circles; monkey 2, gray circles). AS, arcuate sulcus; PS, principal sulcus.

movement on each trial. After the monkeys had maintained fixation (±7.5°) for 1.0 s, a symbolic visual cue appeared in place of the fixation spot. Each cue was a composite of 2 colored ASCII characters (ca. 2.2° each), selected pseudorandomly from a set of 3 such cues, all of which were novel at the beginning of a recording session. The cue lasted for a pseudorandomly selected period of 1.0, 1.5, or 2.0 s. Cue offset served as the trigger ("go") stimulus, after which the monkeys made a saccade to 1 of the 3 potential goals (±7.5°). They were required to continue fixating the chosen goal for 1.0 s, then all 3 targets filled in white and reward might occur 0.5 s later. The reward was a 0.1 mL drop of fluid, but regardless of reward or nonreward, the squares disappeared and the next 2.5-s intertrial interval began.

Figure 1*B* illustrates the types of trials. If, on a given *current trial*, the cue had repeated from the *previous trial* (called *repeat trials*), the monkeys had to choose the same goal as on the previous trial (called a *Repeat-stay strategy*). If, however, the cue had changed from that on the previous trial (called *change trials*), they had to reject the previous goal and choose 1 of the 2 remaining goals (called a *Change-shift strategy*). Because each cue was selected pseudorandomly from a set of 3, 33% of current trials were repeat trials and 67% were change trials. For repeat trials, selection of the strategically correct goal always led to reward. For change trials, rejection of the most recent goal was the only way to gain a reward, but this occurred for only 1 of the 2 strategically correct choices. If a choice was not rewarded—either because of

a strategic error or through choice of the unrewarded option on change trials—a *2nd-chance trial* followed. An unlimited series of 2nd-chance trials repeated the cue until the monkeys obtained a reward.

Surgery

We implanted a 27 × 36 mm recording chamber in an aseptic surgical procedure. Isofluorane anesthesia (1–3%) was used to effect. After making a 27 × 36 mm craniotomy over the right frontal lobe, we implanted titanium bone screws in the surrounding bone and mechanically fixed the recording chamber and a head-restraint device to these screws with methacrylate cement. Postoperative analgesia was given for 3–5 days.

Histological Analysis

Near the end of data collection, we made electrolytic lesions (15 μA for 10 s, anodal current) in selected locations at 2 depths per penetration, with the lesions separated by either 1.5 or 2.0 mm. After approximately 10 days, the animal was deeply anesthetized and then perfused with a 10% (v/v) formol saline. Frozen, coronal sections were Nissl stained and used for architectonic analysis. We plotted the surface projections of the recording sites by reference to the electrolytic lesions and to 5 needles inserted at known coordinates during the perfusion (Fig. 1*C*).

Data Collection Methods

The monkeys' eye position was recorded with an infrared oculometer (Bouis Instruments, Karlsruhe, Germany) at 500–1000 Hz. We used a 16-electrode microdrive with independent control of each electrode (Thomas Recording, Giessen, Germany) to isolate single-unit potentials. Different sites were explored from day to day to build up a population of neurons. Quartz-insulated platinum–iridium electrodes (impedance, 0.5–1.5 MΩ at 1 kHz) provided a signal that was filtered with a band-pass of 0.6–6.0 kHz. The signal was amplified and discriminated with a Multispike Detector (Alpha-Omega Engineering, Nazareth, Israel) or a Multichannel Acquisition Processor (Plexon, Dallas, TX). For the latter, neuronal waveforms were always resorted with Offline Sorter (Plexon). For software, CORTEX (http://www.cortex.salk.edu/) was used to control behavior and collect data.

Data Analysis

We used MatOFF (http://dally.nimh.nih.gov/matoff/matoff.html), SPSS (http://www.spss.com/), and custom software to analyze the data. For the JPETHs, NeuroExplorer (NEX Technologies, Littleton, MA) was used.

For the present analysis, neuron pairs were sampled from 2 neuronal subpopulations, called future-goal (F) cells and previous-goal (P) cells. Details of the single-cell analyses of these subpopulations have been described previously (Genovesio et al. 2006) but are summarized here. Recall that the event sequence involved both current and second-chance trials (Fig. 1*B*). Identifying cells that encoded previous versus future goals depended to a large extent on neural activity during the fixation period, which preceded cue onset on both current and second-chance trials. In both cases, the monkey maintained steady fixation on a light spot for at least 1 s prior to cue onset, and thus sensory and motor factors could be eliminated as factors contributing to neuronal activity. Cells representing previous goals showed spatially tuned activity during the fixation period on current trials, when the monkeys needed that information to choose their next goal. To apply the Change-shift strategy, the previous goal had to be rejected in favor of 1 of the 2 alternatives; to apply the Repeat-stay strategy, the previous goal had to be selected again for the forthcoming saccade. Cells representing future goals showed spatially tuned activity during the fixation period on 2nd-chance trials, when the monkeys had chosen their next goal (Fig. 1*B*, middle). The assumption that the monkeys had chosen their next goal prior to that time was supported by the fact that future-goal cells defined in this way showed comparable properties during current trials (after cue presentation) and during a visuomotor mapping task (Fig. 10 in Genovesio et al. 2006). In the latter task, similar cues instructed a future goal without reference to the Change-shift strategy, the Repeat-stay strategy, or the previous goal.

We applied JPETH analysis to the pairs of simultaneously recorded neurons (Aertsen et al. 1989). This calculation used a median of 181 trials (ranging from 110 to 270 trials). The JPETH is the 2-dimensional cross-correlograms with time versus lag on the abscissa and ordinate and correlation strength on the color axis. The activity from neuron i is represented as $S_i^r(t)$ for the rth trial (Brody 1999). We let $\langle\rangle$ represent averaging over r trials and defined $P_i(t)$ as $\langle S_i^r(t)\rangle$, which is the averaged response or PETH of a neuron i. We then calculated shuffle-corrected covariance matrices, known as *nonnormalized JPETH*, which were defined as

$$J_{i,j}(t_1, t_2)=\langle S_i^r(t_1)S_j^r(t_2)\rangle - P_i(t_1)P_j(t_2).$$

This equation denotes the *raw JPETH* minus a cross product of individual perievent time histograms, known as the *shuffle predictor* (also known as the *PET predictor*). This predictor was calculated by averaging across all possible permutations of the trials and was subtracted from the raw JPETH in order to correct for correlations that originate from covariations excepted from 2 independent, rate-modulated point processes (Palm et al. 1988). Then, to normalize the covariance matrix and obtain a matrix of correlation coefficients, we divided the above equation with the cross product of the time-dependent standard deviations (SDs) of the neurons i and j as follows:

$$J_{Ni,j}(t_1, t_2)=\frac{J_{i,j}(t_1, t_2)}{\sigma_i(t_1)\sigma_j(t_2)}.$$

Correlation coefficients are bounded [−1, 1] in these normalized JPETHs (Aertsen et al. 1989). Because most of the temporal range of correlations was encompassed in a strip of bins near the main diagonal (Vaadia et al. 1995), we plotted the correlations in these bins using a time window of 150 ms along the main diagonal (from lower left). These coincidence histograms were then used for subsequent analyses, including statistical tests. To calculate their confidence intervals, we transformed each correlation coefficient into z value using Fisher's transformation:

$$z^1=\frac{1}{2}\ln\frac{(1+r)}{(1-r)}.$$

In this transformation, z^1 is approximately normally distributed with mean $\frac{1}{2}\ln\frac{(1+\rho)}{(1-\rho)}$ and standard deviation $SD_{z^1}=\frac{1}{\sqrt{n-3}}$. Then, we defined 95% confidence limits as

$$\tanh(z^1 - z_{\alpha/2}SD_{z^1}) < r < \tanh(z^1 + z_{\alpha/2}SD_{z^1}),$$

where n is trial number, and $z_{\alpha/2}$ is 1.96 for a 95% interval.

Statistical tests were computed for the precue fixation period and the minimal cue period, consisting of the 1st 1.0 s after cue onset. We used the assumption that the discharge counts in each raw JPETH bin follow a Poisson distribution, based on the shuffle (PET) predictor, and the periods tested included 27 bins. With Bonferroni correction, the significance level was 0.05/27 = 0.00185. We also tested the possibility that the significant correlations resulted from a few unusual trials. In this test, we divided each set of trials into quartiles and examined the effect of omission of each quartile, taken 1 at a time. If the significant correlation remained after this manipulation, then these pairs were considered to have significant correlations. The onset of significant correlation was defined as the 1st significant bin after the cue onset.

Because cross-correlation analysis could be problematic if the discharge rates are not stationary across repeated trials (Brody 1999), we examined the stationarity of firing rates for all isolated single neurons by evaluating the Z score of their coefficients of variation (CVs) for discharge rates during a 2-s interval aligned on cue onset. The CV of previous- and future-goal cells was similar to that of the other neurons in the sample (Supplementary Fig. 1). However, the firing rates of 3 cells showed relatively high CV values (arrows in Supplementary Fig. 1), indicating that they had a significant lack of stability across trials. Because the lack of stability could cause artifacts in cross-correlation analysis (Brody 1998), we also analyzed the dataset without these 3 neurons. These selective omissions had no effect on the results reported here.

Furthermore, in order to examine a possible artifact from covariations in neuronal excitability (Brody 1999) or variability in task events,

we calculated JPETHs for the example pairs shown below using smaller bins (20 ms). It has been shown that artifacts of those types are more sensitive to changes in bin size than are genuine activity correlations (Brody 1999). The results of this small-bin analysis (Supplementary Fig. 2*A,B*) confirmed the original result. Together with the omission-of-trials manipulation described above, this finding also indicates that the cross-correlations shown here were unlikely to result from artifacts caused by covariations of excitability, trial-to-trial event variability, or nonstationarity.

Another source of artifact in JPETH analysis involves variable neuronal latencies or related temporal factors (Brody 1999). Although our task had 3 different durations for cue period, our statistical test was based on the fixation and minimal cue period, during which monkeys could not know whether the cue would disappear or remain for either an additional 0.5 or 1.0 s. Nevertheless, we examined the JPETH using the trials with 1 duration only and obtained the same result as when all 3 cue durations were included (Supplementary Fig. 3).

Finally, we also computed the time-averaged cross-correlograms (Perkel et al. 1967) for both a broad time range (±2.5 s) and a narrower time range (±100 ms) and compiled population averages for them (Supplementary Fig. 4).

Results

Behavior

The monkeys performed the task very accurately, and the details of these behavioral results have been reported previously (Genovesio et al. 2005). On current trials, the monkeys performed repeat trials at better than 95% correct (96.0% and 96.8% correct for monkeys 1 and 2, respectively), with saccadic reaction times (RTs) of 281 ± 96 ms (SD) and 288 ± 57 ms. On change trials, the monkeys made choices correctly better than 98% of the time (98.3% and 98.9 %), with RTs of 279 ± 93 and 285 ± 47 ms. On 2nd-chance trials, the monkeys performed slightly less accurately but, nevertheless, exceeded 90% correct (92.3% and 93.5%), with RTs of 265 ± 86 and 295 ± 54 ms. The monkeys' oculomotor behavior was reliable, as well (Fig. 2). Although the fixation window was relatively large, the monkey continuously fixated the central spot within a narrow range on successful trials. We confirmed that the trials with saccades of 4° or larger during either the fixation or cue period did not contribute to the correlated activity described below by removing those trials from the analysis (Supplementary Fig. 5).

Database

As monkeys performed the task, we recorded the activity of 1441 isolated single neurons from the prefrontal cortex (Fig. 1*C*), using multiple, moveable microelectrodes. As described in the Materials and Methods, we could identify neurons that encoded either previous or future goals, based on their spatial tuning. In monkey 1, we isolated 742 neurons, of which 59 were previous-goal (P) cells and 64 were future-goal (F) cells. In monkey 2, we studied 699 neurons, including 28 P cells and 20 F cells. As shown in Table 1, the mean firing rate did not significantly differ between F and P cells (Student's *t*-test, t_{168} = 0.47, P = 0.64, nonsignificant [NS]). In addition, the firing rate of F and P cells did not differ significantly from the total neuronal population (1-way analysis of variance [ANOVA], 3 level, F vs. P vs. total population, $F_{2,1437}$ = 1.20, P = 0.30, NS). For the present analysis, we selected P and F cells that had been monitored simultaneously, and the neuronal sample consisted of 42 F–F pairs, 61 F–P pairs, and 33 P–P pairs (36 F–F pairs, 45 F–P pairs, and 24 P–P pairs from monkey 1, with the remainder from monkey 2). Of these pairs, 39 F–F pairs, 57 F–P pairs, and 31 P–P pairs were monitored from different electrodes.

In what follows, we 1st show single-pair examples to validate our JPETH analysis. Then, a population-level analysis follows in order to describe the general properties for each group.

Single-Pair Analysis

Of the F–P pairs, 18% showed significant positive correlations. Figure 3*A* illustrates an example F–P pair with a color code indicating correlated activity and the activity of the individual cells presented as gray histograms along the abscissa and ordinate. In this pair, the future-goal cell's activity appears along the abscissa, with its trial-by-trial activity shown in Figure 3*B*1. The activity of the previous-goal cell is shown along the

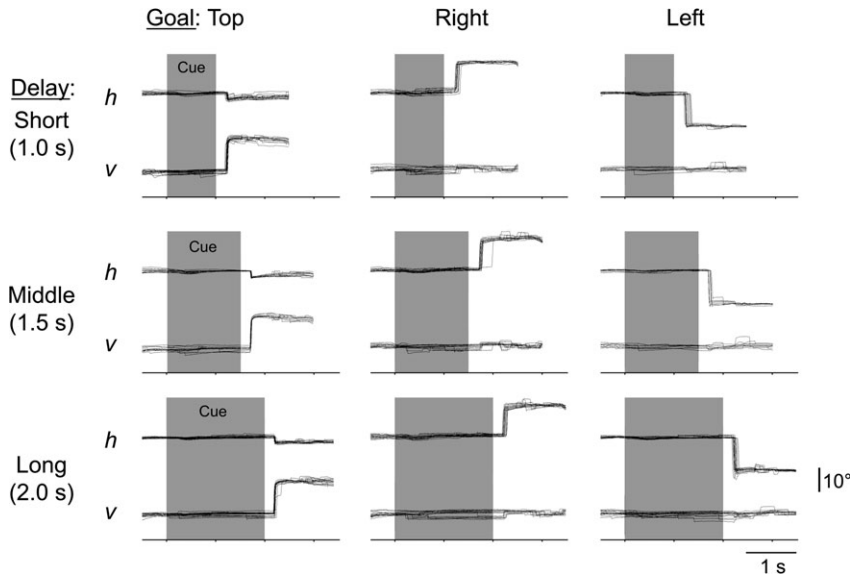

Figure 2. Representative horizontal (*h*) and vertical (*v*) eye position records. Nine combinations of goal locations and cue durations are shown separately. Background shading: cue period.

Table 1
Mean firing rate for each group of cells

	F	P	Rand1	Rand2	Total pop
n	84	87	234	219	1270
Firing rate (sp/s)	3.7	4.0	3.2	3.3	3.3
SD	4.2	4.6	4.7	5.3	5.0

Note: Data from 2 monkeys are combined. Firing rates were calculated using the data from 2-s period from the start of fixation (i.e., including both fixation period and minimal cue period). F and P indicate future- and previous-goal cells, respectively, and Rand1 and Rand2 indicate cells used for each group for random-pair analysis. "Total pop" denotes total population of cells, excluding both F and P cells.

ordinate, with its trial-by-trial activity presented in Figure 3*B*2. The diagonal plot in the right part of Figure 3*A* shows the coincidence histogram, which is also depicted in Figure 3*C*, and the display in the upper right shows the traditional, time-averaged cross-correlogram. The coincidence histogram revealed that the correlated firing of these neurons increased after the appearance of the cue (Fig. 3*A*,*C*). In addition, as shown by aligning the same data on saccade onset, these cells also showed increased correlations during the perisaccade period (Fig. 4). Both cells in this pair were spatially tuned, but their goal preference differed. Specifically, the future-goal cell had its highest discharge rate for the left goal and its lowest for

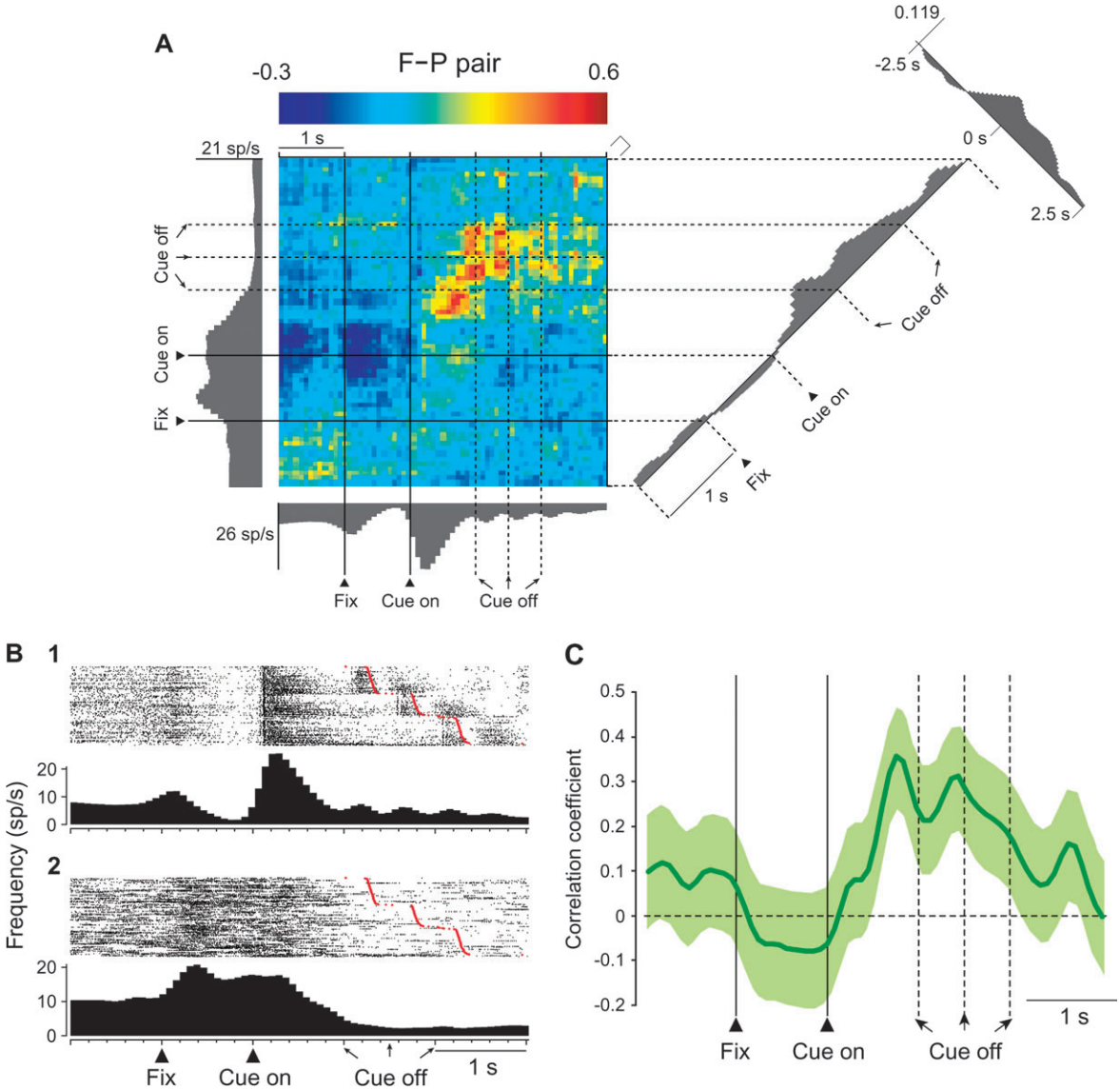

Figure 3. Dynamic modulation of correlated firing in an F–P pair. (**A**) JPETH constructed from 238 trials. The abscissa and ordinate show standard activity histograms for the future-goal (F) cell and the previous-goal (P) cell, respectively. Each pixel of the color-coded matrix displays the normalized correlation coefficient at a particular lag and time delay relative to cue onset: from blue (minimum) to red (maximum). To the right of the JPETH is the coincidence histogram, the correlations along the diagonal from lower left to upper right. It was calculated using a time window of 150 ms oriented perpendicular to that diagonal (marked by the square bracket at the upper right corner of the matrix). Along the time axis of the coincidence histogram, the bin width was 75 ms. The conventional, time-averaged cross-correlogram is shown in the upper right corner (bin width, 75 ms). Total number of spikes used for the JPETH was 25 190; the CV was 81 and 73 for abscissa and ordinate, respectively. The recording session lasted 30.3 min. Fix, onset of fixation; sp, spikes. (**B**) Trial-by-trial activity for the histograms shown on JPETH's axes in (**A**), aligned on cue onset, sorted by saccade onset (red marks). All histograms shown in black or gray were smoothed by a Gaussian filter ($\sigma = 3$ bins). (**C**) The coincidence histogram, equivalent to (**A**), with background shading showing the 95% confidence interval.

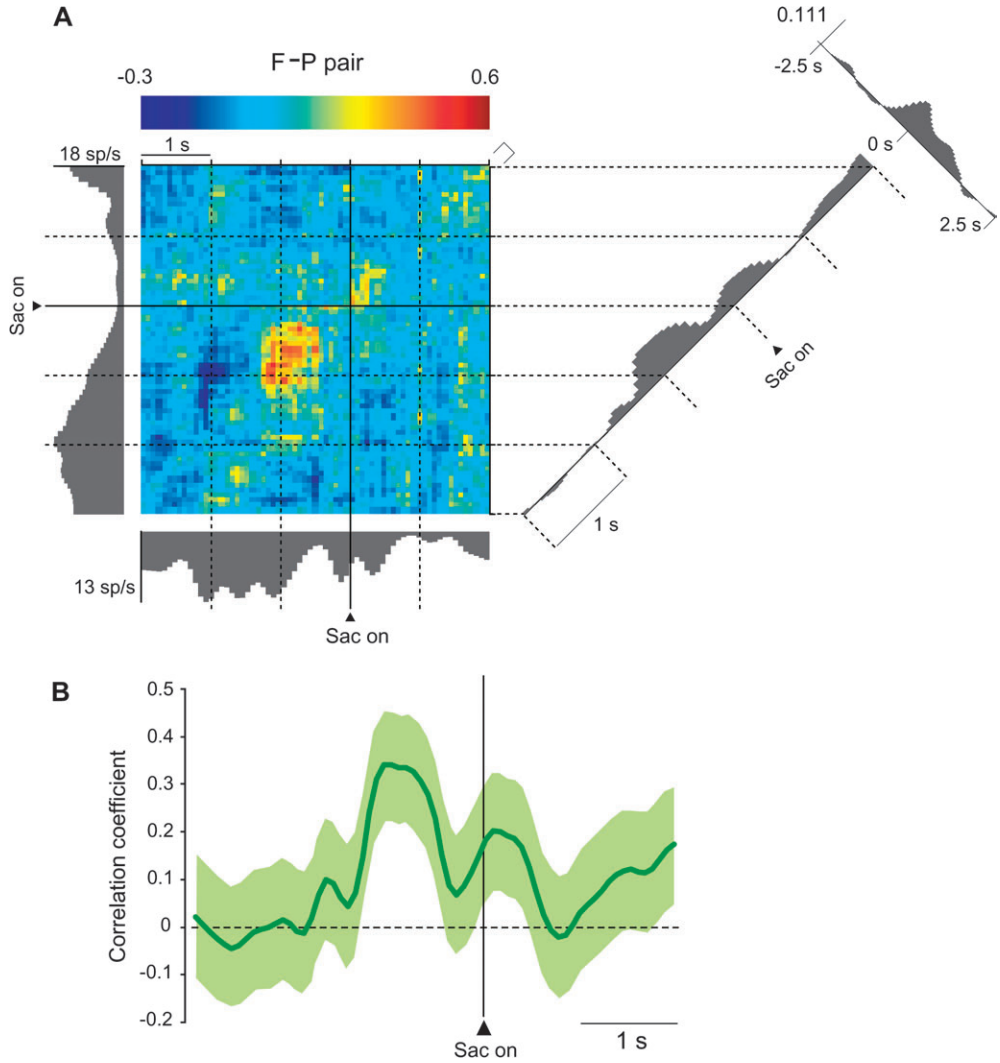

Figure 4. Same F–P pair as in Figure 3, aligned on the saccade (Sac) onset. (**A**) JPETH. Format as in Figure 3*A*. (**B**) Coincidence histogram. Format as in Figure 3*C*.

the right (Supplementary Fig. 6), whereas the previous-goal cell had its greatest discharge rates for goals up and to the right, with the left goal having the least activity (Supplementary Fig. 7). The time-averaged cross-correlograms in Figure 3*A* (upper, right) and Figure 4 (upper, right) show a broad peak in the time range used for this analysis (75-ms bins), but, as shown in Supplementary Figure 4*A*, there was no evidence of rhythmicity or any tightly synchronized activity, as would be seen in 1-ms bins.

In addition to the F–P pairs, 24% of the F–F pairs showed significant positive correlations in activity. Figure 5 illustrates an F–F pair, using 2 different alignment points: cue onset (Fig. 5*A*) and saccade onset (Fig. 5*B*). One future-goal cell in this pair, the one on the abscissa, is the same as the one used for the abscissa of the F–P pair in Figures 3 and 4. The other future-goal cell in Figure 5, the one displayed on the ordinate, had a similar activity pattern and shared the property of having its highest activity for the left goal (Supplementary Fig. 8). The correlation between these cells increased phasically during the fixation period and again after cue onset (Fig. 5*A*), after which it decreased gradually as the saccade time neared (Fig. 5*B*). Like the example F–P pair in Figures 3 and 4, this F–F pair also showed a broad central peak in the time-averaged cross-correlograms (Fig. 5*A,B*), with no evidence of tight synchrony on a millisecond scale (Supplementary Fig. 4*B*).

Although 18% of the F–P pairs and 24% of the F–F pairs showed significant positive correlations, only 3% of the P–P pairs did so, and significant negative correlations were rare for all types of pairs (Fig. 6). Of these correlations, nearly all pairs showed significant, positive correlations for the cue period (73% of the F-P pairs and all the F-F pairs). The proportion of P–P pairs with a significant positive correlation was significantly lower than that of either F–P pairs (χ^2 test, $\chi^2 = 4.33$, degrees of freedom [df] = 1, $P = 0.04$) or F–F pairs ($\chi^2 = 6.38$, df = 1, $P = 0.01$) and did not differ significantly from the proportion expected by chance ($\chi^2 = 0.17$, df = 1, $P = 0.68$, NS). For negative correlations, only 2% of the F–P and 7% of F–F pairs satisfied the criteria for significance, and no P–P pairs did so, also less than or equal to chance levels.

We also evaluated whether significant correlations were more frequent among F–F and F–P pairs than in the general population (Fig. 6). Testing all possible pairs would have been computationally prohibitive, so instead we examined 136 pairs of randomly selected neurons (called the "control" population)

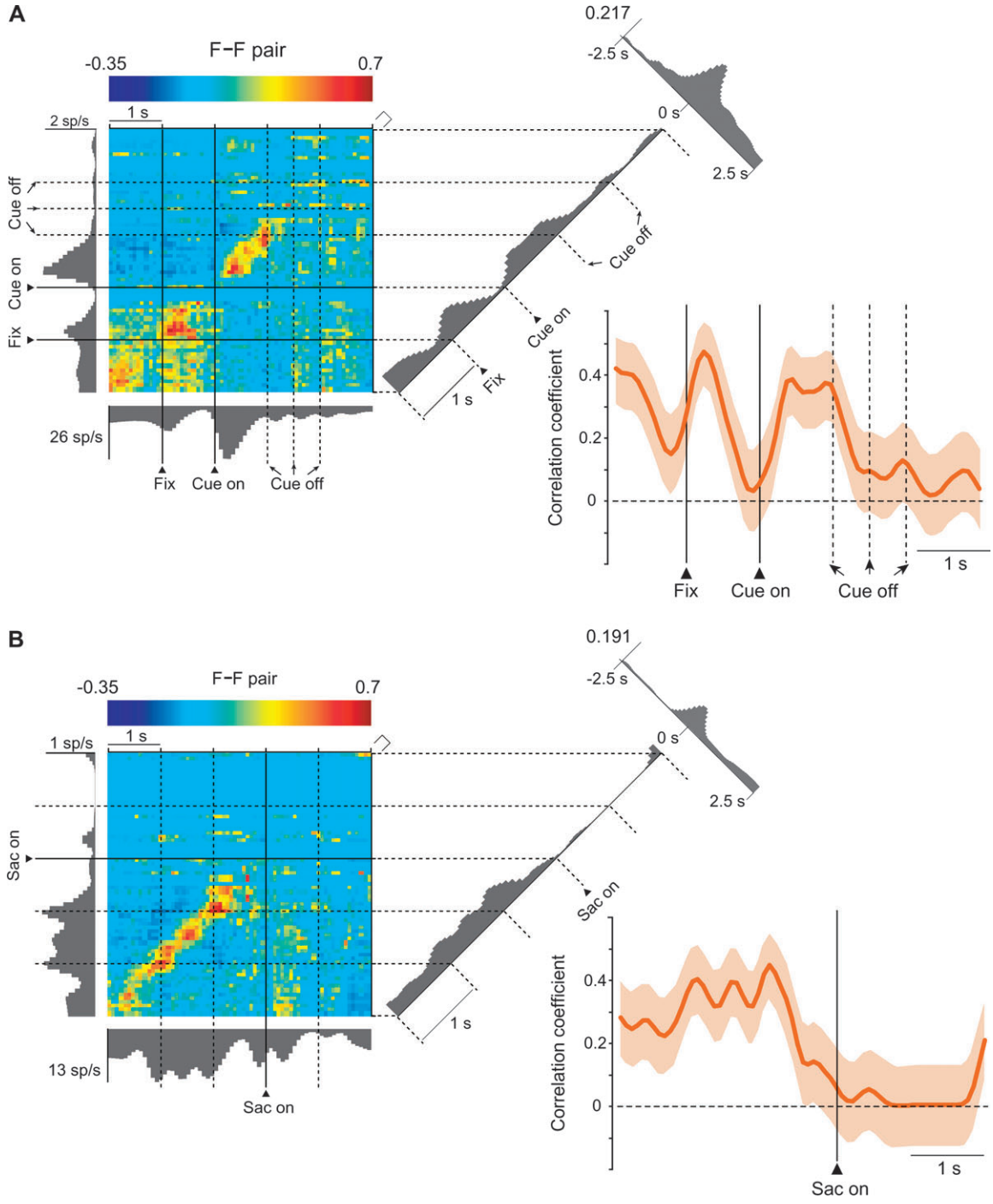

Figure 5. Dynamic modulation of correlated firing in an F–F pair. (**A**) JPETH, coincidence histograms and standard cross-correlation, constructed from 238 trials in the format of Figure 3*A,C*. A total of 11 593 spikes were used; the CV for the ordinate was 167, for the abscissa, 81. The recording session lasted 30.3 min. (**B**) JPETH and coincidence histograms of the same F–F pair as in (**A**) but aligned on saccade (Sac) onset, as in Figure 4. Note that the data in this figure come from the same recording session as do the data illustrated in Figures 3 and 4 and that the figures have 1 cell in common.

that encoded neither future nor previous goals, with the population size chosen to match the sum of the F–F, F–P, and P–P pairs in our database. We performed this test twice using the data from monkey 1, thus generating 2 136-pair datasets. The activity of the control population matched that of the future-goal and previous-goal neurons (Table 1; 1-way ANOVA, 4 level, F vs. P vs. Rand1 vs. Rand2, $F_{3,619} = 0.71$, $P = 0.54$, NS). For the 1st random-pair set, only 10 of 136 pairs (7%) showed significant correlations, and for the 2nd also only 10 of 136 pairs (7%) did so. These percentages were significantly lower than those for F–P and F–F pairs from that monkey (χ^2 test, $\chi^2 = 8.82$, df = 1, $P = 0.003$). The mean number of significant bins was also smaller for the random pairs than for F–P and F–F pairs (2.5 ± 2.0 [SD] and 1.5 ± 0.7 significant bins for the 2 random-pair sets vs. 8.7 ± 7.7 significant bins for F–P and F–F pairs). These differences were also statistically significant (Mann-Whitney

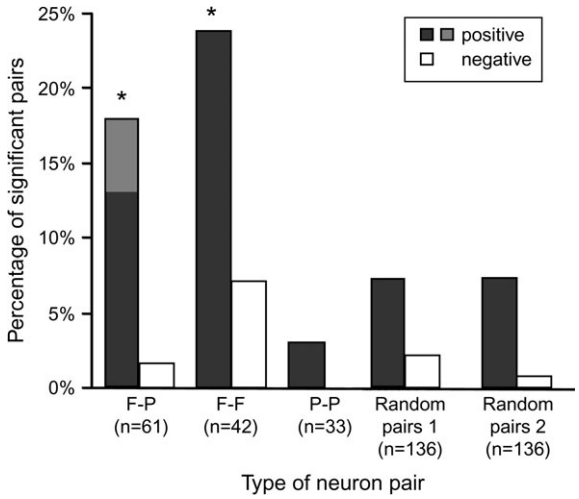

Figure 6. Percentage of pairs showing positive (dark gray bars) and negative (white bars) correlations, based on the correlation during precue fixation period and minimal cue period. Contributions from the fixation period only are filled with lighter shading and involve only the F-P pairs.

U-test, 2 tailed, for the 1st set $n = 10$, $m = 21$, $P = 0.047$; for the 2nd set $n = 10$, $m = 21$, $P = 0.004$). The significantly correlated pairs were observed in both dorsomedial and dorsolateral parts of the prefrontal cortex (Fig. 1*C*) in comparable proportions (χ^2 test, $\chi^2 = 2.13$, df = 1, $P = 0.14$, NS). There was also no areal segregation between F–P and F–F pairs that showed significant correlations ($\chi^2 = 0.69$, df = 1, $P = 0.41$, NS).

Population Analysis

To examine these correlations at a population level, we computed a population average for the coincidence histograms of F–P and F–F pairs with significant, positive correlations (Fig. 7*C*). We also computed population JPETHs, which yielded similar results (Fig. 7*A,B*). Although the population JPETH shown in Figure 7*A,B* are unweighted average across populations, we also computed weighted averages so that all pairs contribute equally (maximal correlation set to 1.0), and this analysis yielded similar results. Consistent with the single-pair examples illustrated in Figures 3–5, these populations of pairs increased their correlations after the cue appeared and remained relatively stable until the cue disappeared (Fig. 7*A–C*). The onset of this increase was 355 ± 225 (SD) ms for F–P pairs and 353 ± 265 ms for F–F pairs. Later, the correlation in F–F pairs decreased prior to the onset of the saccade, whereas that in F–P pairs remained relatively high during the saccade and while the goal was fixated (Fig. 7*C*, arrow). In addition, F–F pairs also showed a phasic increase in correlated activity during the 1st part of the fixation period.

As illustrated in Figure 8*A*, the mean correlation coefficient during the cue period was significantly higher during change trials than during repeat trials for both F–F and F–P pairs (Wilcoxon signed rank test, for F–F pairs, $n = 10$, $P = 0.003$; for F–P pairs, $n = 11$, $P = 0.02$). These correlations could not have been due to firing rate effects. The mean rate of activity did not differ on change trials compared with repeat trials. For change trials, mean activity was 4.0 ± 4.7 spikes/s, and for repeat trials it was 3.8 ± 4.3 spikes/s (Student's *t*-test, $t_{338} = 0.46$, $P = 0.64$, NS).

Notwithstanding computations based on the shuffle (PET) predictor, it has been reported that cross-correlations between 2 neurons tend to increase with neuronal firing rate (de la Rocha et al., 2007). To examine this possibility, we compared the population coincidence histogram with the average activity histograms for the neurons composing the F-P (Fig. 7*D*) and F-F pairs (Fig. 7*E*). The result shows that there was no clear relationship between firing rate and correlation. It nevertheless might be argued that, for F-F pairs, the correlations would be expected to be high when future goals were being encoded because its component neurons would have been discharging or nearing the threshold for discharge at those times. The same expectation would hold, however, for P-P pairs, which discharged in relation to previous goals, yet significant correlations among these cells were rarely observed (Fig. 6).

To examine other potential interpretational problems, we constructed separate population coincidence histograms to eliminate certain factors as substantial contributors to the present results. One of these factors was a population composed exclusively of pairs monitored from different electrodes. For the most part, individual neurons in each pair analyzed in this report were recorded simultaneously from different electrodes. We also recorded neuron pairs monitored from the same electrode, but these data were analyzed separately because of potential artifacts for 2 neurons recorded from a single electrode (Bar-Gad et al. 2001). We included these neurons in the present analysis but adopted the policy that any result or conclusion presented here must be valid in the absence of these pairs. Supplementary Figure 9*A* confirms that removal of these single electrode pairs had virtually no effect on the population averages compared with Figure 7*C*.

A 2nd factor involved pair selection. We ruled out multiple test effects in the main analysis by Bonferroni correction. We checked this method by contrasting the number of significant bins in F and P cell pairs. This number was then compared with a random selection of other neurons, and pairs were included in the population based on an assessment of the probability of observed counts in each bin of the raw JPETH ($\alpha = 0.05$) of a given F or P pair, relative to the random pairs. A population selected on this basis, without Bonferroni correction, showed virtually the same properties as the population with this correction (Supplementary Fig. 9*B* vs. Fig. 7*C*).

Finally, in the plots and analysis presented thus far, we included both the current and 2nd-chance trials in the analysis. To examine the influence of 2nd-chance trials in the averages, we eliminated those trials from the analysis, leaving current trials only (Supplementary Fig. 10). Although the F-F pairs' fixation period correlation was smaller in the absence of 2nd-chance trials (Supplementary Fig. 10*B,C*), the overall pattern of results was similar for the F-P (Supplementary Figs 9 and 10*A,C*) and F-F pairs (Supplementary Fig. 10*B,C*).

We mentioned above that population coincidence histograms were consistent with the single-pair examples illustrated in Figures 3–5. In addition, as shown in Supplementary Figure 4, population averages for the time-averaged cross-correlograms were also consistent with the single-pair examples. The pair illustrated in Figures 3 and 4 appears in Supplementary Figure 4*A*, and the pair from Figure 5 is illustrated in Supplementary Figure 4*B*, both computed for a narrow (1 ms) bin width. Neither pair showed sharp synchrony, and population-averaged cross-correlograms in the millisecond range similarly failed to

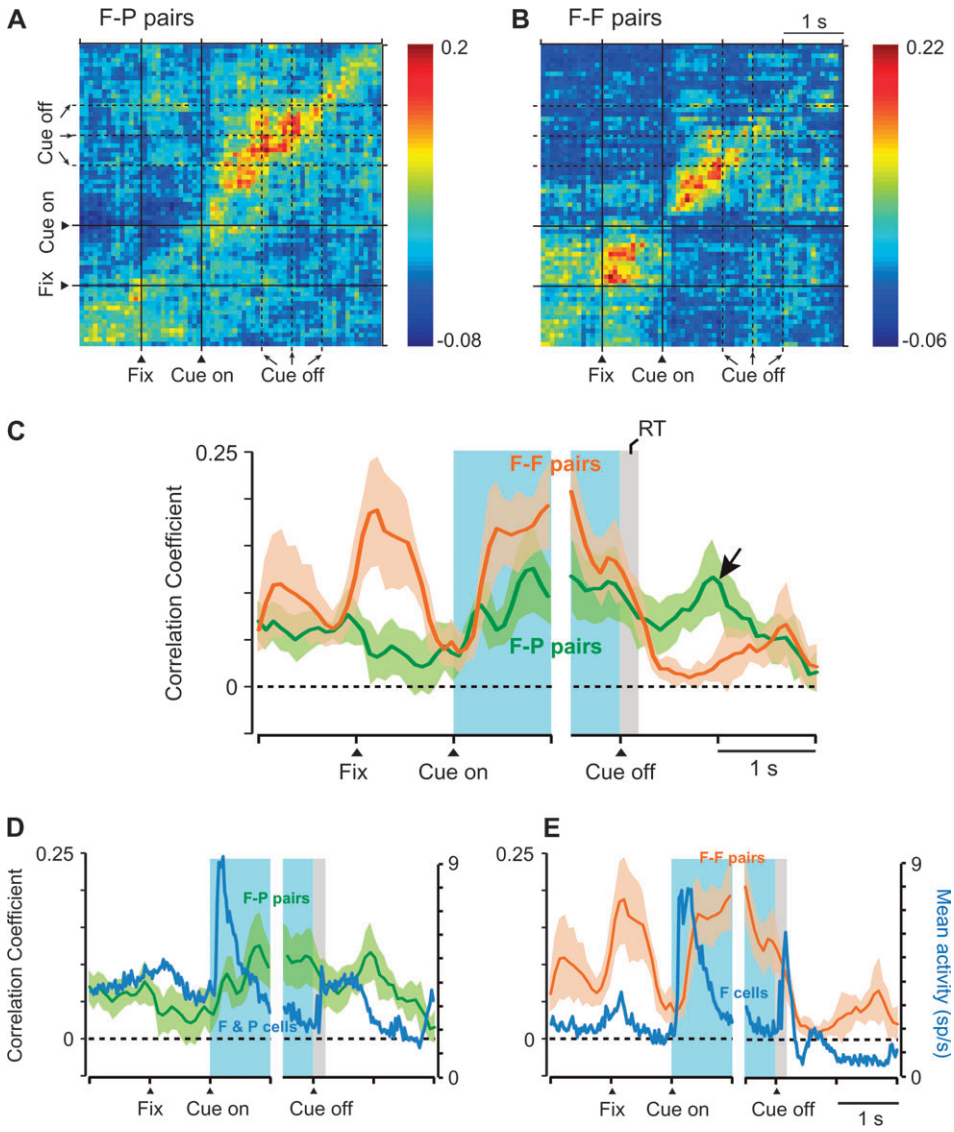

Figure 7. Population analysis. (**A**) Population average of JEPTHs for F–P pairs with significant positive correlations ($n = 11$). (**B**) As in (**A**), for F–F pairs ($n = 10$). (**C**) Population-averaged coincidence histograms, calculated from neuron pairs with significant, positive correlations ($n = 11$ for F–P pairs, $n = 10$ for F–F pairs). Coincidence histograms for individual pairs were calculated as in Figure 3*A,C* but without smoothing. These histograms were then averaged bin by bin across each subpopulation and smoothed using a moving average of 3 bins. Background shading shows standard error of the mean. The arrow marks a period after the goal had been chosen and acquired, but feedback had not yet arrived. Note that the plot is divided into 2 parts, 1 aligned on cue onset and the other on cue offset, because the duration of the cue was variable and unpredictable. (**D**) Population average activity of all future- and previous-goal cells composing the significantly correlated F–P pairs (blue line), shown together with the coincidence histogram of F–P pairs from (**C**). (**E**) In the format of (**D**), for F-F pairs and the future-goal cells composing those pairs. Fix, onset of fixation.

reveal such a property (Supplementary Fig. 4*C*). For a broad time range (±2.5 s), both F–P and F–F pairs showed wide, single peaks around time zero (Supplementary Fig. 4*D*). No rhythmic activity was observed in either time range at either the population or single-pair level.

As mentioned above, an important feature of the individual future- and previous-goal cells is that they showed spatial tuning. We examined whether the members of F–F and F–P pairs shared the same preferred goal, defined as the goal associated with the highest firing rate. If preferred goals were equally distributed, then neuron pairs with different preferred goals should outnumber those with the same one by a ratio of 2:1. Neuron pairs lacking significant correlations did not differ significantly from this ratio (Fig. 8*C*; χ^2 test for F-P pairs, $\chi^2 = 0.33$, df = 1, $n = 50$, $P = 0.56$, NS; for F–F pairs, $\chi^2 = 0.12$, df = 1, $n = 32$, $P = 0.73$, NS). Likewise, the preferred goal of neurons in F–P pairs with significant correlations failed to differ from the chance ratio of 2:1 (Fig. 8*B*, left; χ^2 test, $n = 11$, $\chi^2 = 0.10$, df = 1, $P = 0.76$, NS). Only F–F pairs with significant correlations were significantly more likely to share the same preferred goal (Fig. 8*B*, right): compared with chance ($\chi^2 = 4.43$, df = 1, $n = 10$, $P = 0.04$), with F–P pairs with significant correlations ($\chi^2 = 5.84$, df = 1, $P = 0.02$), or with F–P ($\chi^2 = 9.70$, df = 1, $P = 0.002$), or with F–F pairs ($\chi^2 = 5.52$, df = 1, $P = 0.02$) lacking significant correlations.

Discussion

The prefrontal cortex has been viewed as a neural substrate for selecting and representing goals, including those based on

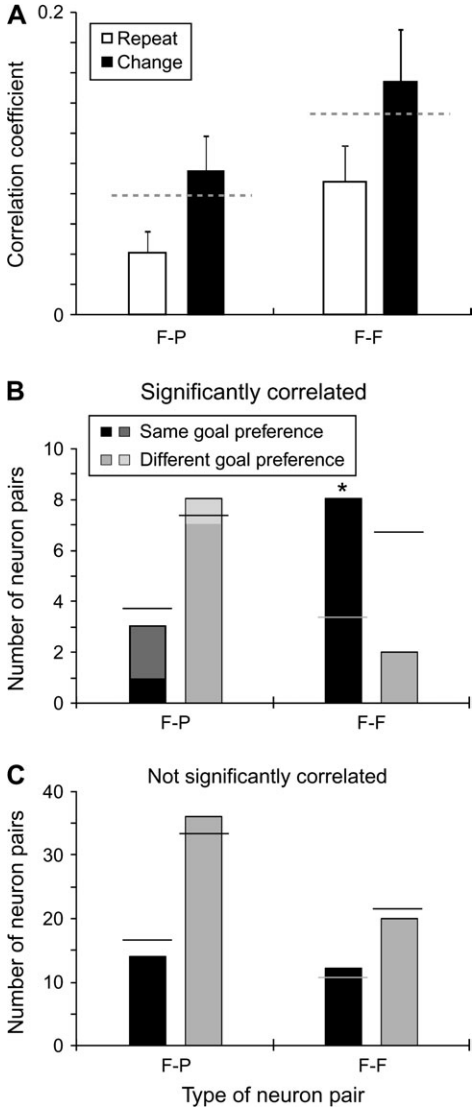

Figure 8. (**A**) Mean correlation coefficients for repeat- and change trials, calculated from 0–1.0 s after cue onset. Gray dashed lines show the mean values for the F–P pairs (left) and F–F pairs (right), matching the values in Figure 7*C* for the cue period. Error bars show standard error of the mean. (**B, C**) Number of neuron pairs in which individual cells had the same or different preferred goals. (**B**) Pairs with significant positive correlations. Horizontal lines show the values expected by the chance. Contributions from the fixation period only are filled with lighter shading, and involve only the F-P pairs. (**C**) In the format of (**B**), for pairs without significant positive correlations.

high-order rules and strategies (Owen et al. 1996; Rowe et al. 2000; Rowe and Passingham 2001; Gaffan et al. 2002; Bunge 2004). The current study revealed several features of discharge correlations during goal selection and maintenance in the abstract strategy task of Genovesio et al. (2005): 1) as monkeys chose a goal, F–P and F–F pairs often showed significant correlations during the cue period, but P–P pairs rarely did so (Fig. 6); 2) both F–P and F–F pairs showed enhanced correlations during the cue period, when the monkeys selected and maintained a goal (Fig. 7*C*), and F–P pairs maintained these correlations at a stable level after goal acquisition (Fig. 7*C*, arrow); 3) in F–P pairs with significant correlations, the members of the pair rarely shared goal preferences during the cue period, but in F–F pairs they commonly did so (Fig. 8*B*); 4) correlations among members of a pair were greater during change trials, when the monkeys rejected the previous goal, than during repeat trials, when the monkeys selected the previous goal again (Fig. 8*A*); and 5) these correlations lack rhythmicity or sharp synchrony (Supplementary Fig. 4*C*).

Potential Functional Contributions

The analytical method used here assessed the likelihood that spikes from 2 neurons fell into the same time bin, beyond that expected simply from their discharge rates. In the past, these transient correlations have been interpreted in terms of net changes in neuronal interactions, particularly through recurrent, excitatory loops that could sustain persistent neuronal activity (Amit et al. 1994; Amit and Brunel 1997; Camperi and Wang 1998; Wang 2001; Constantinidis and Wang 2004). Alternatively, such correlations can occur with sparse, if any, synaptic connections between cells (Vaadia et al. 1995). We discuss below some potential sources of the correlations but focus here on their possible functional significance. Transient correlations, regardless of their cause, could make the outputs from the 2 neurons of a pair more efficacious, especially if their efferents converge on target neurons. Paz et al. (2007), for example, showed that correlated activity promoted the transfer of information from one cortical area to another—in that study from the entorhinal cortex to the perirhinal cortex. Accordingly, we discuss the possible functional significance of each kind of pair, in turn, in the context of this assumption. We note that future goals were also movement targets, so we cannot distinguish between spatial goals and motor commands.

In accord with current thinking about short-term memory mechanisms, the correlated activity of F–F pairs could contribute to the selection and active maintenance of future-goal representations (Amit et al. 1994; Camperi and Wang 1998; Compte et al. 2000), especially for F-F pairs with similar goal preferences. On this view, the correlations support the maintenance of persistent discharge that represents a future goal. Recurrent, excitatory interactions could play a role in supporting such activity (Amit and Brunel 1997; Camperi and Wang 1998; Wang 2001; Constantinidis and Wang 2004), but it is not necessary to invoke such a mechanism (Vaadia et al. 1995). Regardless of the cause of the correlation, if the pairs' outputs converge on target neurons, then temporal summation should enhance the efficacy of those efferents. Assuming further that these cells project to networks that transform a prospective coding signal into action, temporal and spatial summation would make correlated F–F pairs more effective than uncorrelated pairs in this computation. The finding that F–F pairs showed a marked decrease in their correlations after goal attainment (Fig. 7*C*) is also consistent with their role in prospective coding. F–F pairs also showed enhanced correlations after the onset of fixation, prior to the cue (Fig. 7*B,C*, Supplementary Fig. 10*B,C*), when a goal could not yet have been selected. This increased correlation is difficult to understand, but if within-pair correlations enhance the efficacy of their neuronal outputs, they could contribute to activating the representations of potential motor commands, which—once the precue fixation period begins—consist solely of saccades to the 3 potential response goals.

As for F–P pairs, after cue presentation their correlations roughly matched those for F–F pairs during the cue period (Fig. 7*C*). The presence of these correlations and their time course suggest that the correlations in these pairs, too, contribute to

the selection and maintenance of spatial goals. Recall that, like F-F pairs, F-P pairs showed greater correlations during change trials, when the previous goal should be rejected in favor of an alternative, than during repeat trials (Fig. 8*A*). Unlike F-F pairs, however, the members of F–P pairs usually encoded different goals (Fig. 8*B*). Recall also the relationship between future- and previous goals. At the start of a current trial, the previous goal is the one most recently selected and acquired. The future goal is the one selected and acquired during a current trial. If that choice does not produce a reward, a 2nd-chance trial ensues in which the monkeys must choose the least recently acquired goal (Fig. 1*B*). To perform the 2nd-chance trial correctly, the monkeys must remember and eliminate both the goal chosen on the previous trial and the goal chosen on the just ended "current trial." The discharge activity of F-P pairs represents just this combination of goals. If, as assumed above, correlated activity makes convergent efferents from these neurons more efficacious, then the correlations in F–P pairs could enhance their ability to signal these 2 most recently selected goals to the networks that choose the goal on second-chance trials. The observation that F–P pairs maintained an enhanced level of correlations after goal acquisition, which diminished once feedback arrived (Fig. 7*C*, arrow), also agrees with this hypothesis because the choice on 2nd-chance trials occurs at this time. On this view, both the spikes and their correlations would be important in suppressing the repetition of prior choices. Prefrontal cortex lesions cause perseverative errors in tasks requiring the shifting of rules, task sets, or responses (Passingham 1972; 1985; Dias et al. 1997; Collins et al. 1998), and both spikes and correlations could contribute to the behavioral flexibility that characterizes the behavior of primates with intact frontal lobes. Alternatively, the correlated activity in F-P pairs could also reflect a monitoring function.

The paucity of significant P–P correlations, together with the presence of many such correlations among F–P pairs, suggests that retrospective information in the prefrontal cortex, as encoded by the previous-goal cells, is most important for prospective coding, rather than in memory maintenance or working memory per se. Neuroimaging (Owen et al. 1996; Cohen et al. 1997; Postle et al. 1999; Rowe et al. 2000; Rowe and Passingham 2001; Fletcher and Henson 2001) and neuro-computational (Rougier et al. 2005; O'Reilly 2006; O'Reilly and Frank 2006) studies point in the same direction. For example, Owen et al. (1999) showed that the middorsolateral prefrontal cortex is involved more in the performance of a 2 back memory task, which required the subject to continually update and manipulate the stored sequence of spatial locations, than in a spatial span task, in which the subject had only to hold a sequence of locations in memory. In line with this finding, Bor et al. (2003) demonstrated that the dorsolateral prefrontal cortex increased its activity when subjects reorganized the items retained in short-term memory into higher level groupings or "chunks," compared with a condition in which such grouping did not occur, notwithstanding the fact that successful grouping decreased memory demands. Based on these and other findings, Owen et al. (2005) concluded that the dorsolateral prefrontal cortex contributes to the strategic control of contents that are held in working memory, thereby facilitating subsequent processing for future decisions and actions. The paucity of significant P–P correlations agrees with these ideas about prefrontal cortex function and provide further systems-level support for them.

Relation to Previous Studies

Several previous studies have reported cell-to-cell correlations in the prefrontal cortex within the range of a few milliseconds (Abeles et al. 1995; Rao et al. 1999; Constantinidis et al. 2001; Constantinidis and Goldman-Rakic 2002; Sakurai and Takahashi 2006). A study using a spatial delayed response task reported that prefrontal cortex neurons were more likely to show cross-correlation peaks if they shared similar functional properties, including spatial preferences (Constantinidis et al. 2001). The F–P correlations reported here provide evidence that cells can show significant correlations without sharing similar spatial preferences (Fig. 8*B*) or other key functional properties, such as retrospective versus prospective coding. The present findings also show that cells sharing spatial preferences might show significant correlations, as was typically the case for F–F pairs, or might not, as in F–P pairs, depending on their other properties (Fig. 8*B*). In another recent study, Sakurai and Takahashi (2006) showed that synchrony among prefrontal cortex neurons changed dynamically depending on the tasks and events being processed. In the present data, dynamic changes in correlation depended not only on those factors but also on the specific properties of the cells composing a pair (e.g., F–P vs. F–F pairs). The present results extend previous work on transient correlations and related measures by focusing on cells with specific properties related to the selection and maintenance of goals based on abstract response strategies.

Nature of the Correlations

We emphasize that the present study found relatively "loose" or "broad" synchrony, in the range of tens to hundreds of milliseconds, as opposed to "tight," "sharp," or "narrow" synchrony, in the order of milliseconds (Supplementary Fig. 4*A–C*). The broad correlation functions we observed have been reported in several previous studies (Gochin et al. 1991; Nelson et al. 1992; Eggermont 1992; Vaadia et al. 1995; Nowak et al. 1999; Katz et al. 2002; Narayanan and Laubach 2006) and seem to be a different phenomenon from previously reported, tight synchrony in prefrontal cortex (Constantinidis et al. 2001; Sakurai and Takahashi 2006). We note, however, that Vaadia et al. (1995) reported both tight and loose synchrony in the same frontal population, as have others elsewhere (Gochin et al. 1991; Hata et al. 1991; Nelson et al. 1992; Eggermont 1992; Nowak et al. 1995, 1999), and our results confirm the latter. A possible factor that could have contributed to the lack of sharp synchrony in our data was the distance between cells in a pair. For example, Katz et al. (2002) showed that narrower cross-correlation peaks tend to be observed in nearby neurons, whereas broader peaks tend to be observed in widely separated neurons, including in neuron pairs from different hemispheres. Likewise, Nowak et al. (1999) examined cross-correlations between distantly located neurons in areas V1 and V2 of monkeys and reported that they rarely (<1%) showed sharp synchrony. Many of their pairs, however, showed broad cross-correlation peaks, in the order of hundreds of milliseconds to seconds. Consistent with these findings, Constantinidis and Goldman-Rakic (2002) showed that sharp correlation peaks were difficult to observe beyond 0.2 mm. This conclusion is consistent with the fact that the minimal distance between our electrodes was 0.5 mm, without considering the additional separation caused by differences in depth. (Unfortunately,

more detailed analysis of the relationship between neuronal separation and JPETH correlations could not be performed on the present data for technical reasons.) Additionally, in typical cross-correlation studies, there has been a focus on narrow time windows, such as cue or delay periods, whereas in our JPETH analysis, we included a much longer period, which contributed substantially to the broad correlation peaks that we observed.

Thus, the correlations reported here are most likely to have resulted from polysynaptic interactions and indirect common input (Nowak et al. 1995) and not from the direct, monosynaptic connections. Polysynaptic interactions could also account for the lack of rhythmic activity in our data. Although rhythmicity might be expected among neurons in a recurrent network, such activity is likely to be decayed or desynchronized through several synapses between neurons in a pair or between them and their common inputs. This possibility was especially likely because, as noted above, our electrodes were separated by relatively long distances compared with other studies (Constantinidis et al. 2001; Sakurai and Takahashi 2006). Furthermore, we assume that those cells participate in several networks (Izhikevich et al. 2004; Rougier et al. 2005), which could also mask rhythmic activity. Another contribution to the dynamic correlations could be modulation of firing rate, notwithstanding the computational approach used in JPETH analysis to account for this factor through the shuffle (PET) predictor (de la Rocha et al. 2007). However, correlations in the F–P pairs do not seem to be dependent on firing rate because the maximum correlation is observed during intervals of lower firing rate (Fig. 7*D*). Likewise, correlations in F–F pairs correspond poorly to the change in firing rate in future-goal cells (Fig. 7*E*). Thus, the correlations observed here are unlikely to be accounted for simply by the rate modulations.

Possible Oculomotor Influences

An important interpretational issue concerns the possible effects of eye movement on the correlated activity. Although the monkeys did not make many standard saccades during the fixation period (Fig. 2), either before the cue or after goal acquisition, small number of saccades and/or random microsaccades could, in principle, have affected the present results. This contaminant was unlikely, however, because: 1) the visual or motor fields previously reported for cells in these areas are large, >10 degrees (Mikami et al. 1982; Suzuki and Azuma 1983), which makes it unlikely that small eye movements will bring a stimulus into and out of such a field; 2) a previous study regarding cross-correlations in these areas ruled out increases in correlation due to microsaccades (Constantinidis and Goldman-Rakic 2002); 3) whereas the microsaccades appear to occur randomly, the correlated activity observed here increased after the cue appeared; and 4) removal of the trials that included saccades in excess of 4° did not influence the present findings (Supplementary Fig. 5).

Conclusions

The present data indicate that transient correlations among prefrontal cortex neurons, specifically those encoding previous and future goals, contribute to goal selection and maintenance. Along with classic neurological thinking, recent experimental work supports goal selection and maintenance as a central function of prefrontal cortex (Owen et al. 1996; Rowe et al. 2000; Rowe and Passingham 2001; Gaffan et al. 2002; Saito et al. 2005; Mushiake et al. 2006). In accord with some of these theories of prefrontal cortex function, its contribution becomes most pronounced when previous goals or task sets need to be rejected in favor of an alternative (e.g., Owen et al. 1993; Wise et al. 1996). Although the present task was operantly conditioned (Genovesio et al. 2005), monkeys spontaneously adopt the same strategies as they learn symbolically guided actions (Wise and Murray 1999), and humans use similar strategies. Indeed, daily life activities depend to a considerable extent on choosing new goals based on what has already been accomplished. Failure of the neural mechanisms described here—the loss of correlations within cell assemblies that should make their outputs more efficacious—could contribute to the deficits of goal omission or perseveration that characterize dementia and obsessive-compulsive disorder, which have been linked to frontal lobe dysfunction.

Supplementary Material

Supplementary material can be found at: http://www.cercor.oxfordjournals.org/.

Funding

Intramural Research Program of the National Institutes of Health, National Institute of Mental Health (Z01MH-01092-29). Japan Society for the Promotion of Science (research fellowship to S.T.).

Notes

We thank Mr Alex Cummings for preparing the histological material. We also thank Drs Rony Paz, Tim Buschman, and Markus Siegel and 4 anonymous referees for constructive comments and suggestions. *Conflict of Interest*: None declared.

Address correspondence to Satoshi Tsujimoto, Laboratory of Systems Neuroscience, National Institute of Mental Health, Building 49, Room B1EE17, 49 Convent Drive, MSC 4401, Bethesda, MD 20892-4401, USA. Email: tsujimotos@mail.nih.gov.

References

Abeles M, Bergman H, Gat I, Meilijson I, Seidemann E, Tishby N, Vaadia E. 1995. Cortical activity flips among quasi-stationary states. Proc Natl Acad Sci USA. 92:8616–8620.

Aertsen AM, Gerstein GL, Habib MK, Palm G. 1989. Dynamics of neuronal firing correlation: modulation of "effective connectivity. J Neurophysiol. 61:900–917.

Amemori K, Sawaguchi T. 2006. Rule-dependent shifting of sensorimotor representation in the primate prefrontal cortex. Eur J Neurosci. 23:1895–1909.

Amit DJ, Brunel N. 1997. Model of global spontaneous activity and local structured activity during delay periods in the cerebral cortex. Cereb Cortex. 7:237–252.

Amit DJ, Brunel N, Tsodyks MV. 1994. Correlations of cortical Hebbian reverberations: theory versus experiment. J Neurosci. 14:6435–6445.

Bair W, Zohary E, Newsome WT. 2001. Correlated firing in macaque visual area MT: time scales and relationship to behavior. J Neurosci. 21:1676–1697.

Bar-Gad I, Ritov Y, Vaadia E, Bergman H. 2001. Failure in identification of overlapping spikes from multiple neuron activity causes artificial correlations. J Neurosci Methods. 107:1–13.

Bor D, Duncan J, Wiseman RJ, Owen AM. 2003. Encoding strategies dissociate prefrontal activity from working memory demand. Neuron. 37:361–367.

Brody CD. 1998. Slow covariations in neuronal resting potentials can lead to artefactually fast cross-correlations in their spike trains. J Neurophysiol. 80:3345–3351.
Brody CD. 1999. Correlations without synchrony. Neural Comput. 11:1537–1551.
Brown EN, Kass RE, Mitra PP. 2004. Multiple neural spike train data analysis: state-of-the-art and future challenges. Nat Neurosci. 7:456–461.
Bunge SA. 2004. How we use rules to select actions: a review of evidence from cognitive neuroscience. Cogn Affect Behav Neurosci. 4:564–579.
Camperi M, Wang XJ. 1998. A model of visuospatial working memory in prefrontal cortex: recurrent network and cellular bistability. J Comput Neurosci. 5:383–405.
Cohen JD, Perlstein WM, Braver TS, Nystrom LE, Noll DC, Jonides J, Smith EE. 1997. Temporal dynamics of brain activation during a working memory task. Nature. 386:604–608.
Collins P, Roberts AC, Dias R, Everitt BJ, Robbins TW. 1998. Perseveration and strategy in a novel spatial self-ordered sequencing task for nonhuman primates: effects of excitotoxic lesions and dopamine depletions of the prefrontal cortex. J Cogn Neurosci. 10:332–354.
Compte A, Brunel N, Goldman-Rakic PS, Wang XJ. 2000. Synaptic mechanisms and network dynamics underlying spatial working memory in a cortical network model. Cereb Cortex. 10:910–923.
Constantinidis C, Franowicz MN, Goldman-Rakic PS. 2001. Coding specificity in cortical microcircuits: a multiple-electrode analysis of primate prefrontal cortex. J Neurosci. 21:3646–3655.
Constantinidis C, Goldman-Rakic PS. 2002. Correlated discharges among putative pyramidal neurons and interneurons in the primate prefrontal cortex. J Neurophysiol. 88:3487–3497.
Constantinidis C, Wang XJ. 2004. A neural circuit basis for spatial working memory. Neuroscientist. 10:553–565.
de la Rocha J, Doiron B, Shea-Brown E, Josić K, Reyes A. 2007. Correlation between neural spike trains increases with firing rate. Nature. 448:802–806.
Dias R, Robbins TW, Roberts AC. 1997. Dissociable forms of inhibitory control within prefrontal cortex with an analog of the Wisconsin Card Sort Test: restriction to novel situations and independence from "on-line" processing. J Neurosci. 17:9285–9297.
Eggermont JJ. 1992. Neural interaction in cat primary auditory cortex. Dependence on recording depth, electrode separation, and age. J Neurophysiol. 68:1216–1228.
Engel AK, Fries P, Singer W. 2001. Dynamic predictions: oscillations and synchrony in top-down processing. Nat Rev Neurosci. 2:704–716.
Fletcher PC, Henson RN. 2001. Frontal lobes and human memory: insights from functional neuroimaging. Brain. 124:849–881.
Fukushima T, Hasegawa I, Miyashita Y. 2004. Prefrontal neuronal activity encodes spatial target representations sequentially updated after nonspatial target-shift cues. J Neurophysiol. 91:1367–1380.
Funahashi S, Bruce CJ, Goldman-Rakic PS. 1989. Mnemonic coding of visual space in the monkey's dorsolateral prefrontal cortex. J Neurophysiol. 61:331–349.
Fuster JM, Alexander GE. 1971. Neuron activity related to short-term memory. Science. 173:652–654.
Gaffan D, Easton A, Parker A. 2002. Interaction of inferior temporal cortex with frontal cortex and basal forebrain: double dissociation in strategy implementation and associative learning. J Neurosci. 22:7288–7296.
Genovesio A, Brasted PJ, Mitz AR, Wise SP. 2005. Prefrontal cortex activity related to abstract response strategies. Neuron. 47:307–320.
Genovesio A, Brasted PJ, Wise SP. 2006. Representation of future and previous spatial goals by separate neural populations in prefrontal cortex. J Neurosci. 26:7305–7316.
Gochin PM, Miller EK, Gross CG, Gerstein GL. 1991. Functional interactions among neurons in inferior temporal cortex of the awake macaque. Exp Brain Res. 84:505–516.
Hasegawa R, Sawaguchi T, Kubota K. 1998. Monkey prefrontal neuronal activity coding the forthcoming saccade in an oculomotor delayed matching-to-sample task. J Neurophysiol. 79:322–333.
Hata Y, Tsumoto T, Sato H, Tamura H. 1991. Horizontal interactions between visual cortical neurones studied by cross-correlation analysis in the cat. J Physiol. 441:593–614.
Hebb DO. 1949. The organization of behavior: a neuropsychological theory. Wiley: New York.
Izhikevich EM, Gally JA, Edelman GM. 2004. Spike-timing dynamics of neuronal groups. Cereb Cortex. 14:933–944.
Jackson A, Gee VJ, Baker SN, Lemon RN. 2003. Synchrony between neurons with similar muscle fields in monkey motor cortex. Neuron. 38:115–125.
Katz DB, Simon SA, Nicolelis MAL. 2002. Taste-specific neuronal ensembles in the gustatory cortex of awake rats. J Neurosci. 22:1850–1857.
Kim JN, Shadlen MN. 1999. Neural correlates of a decision in the dorsolateral prefrontal cortex of the macaque. Nat Neurosci. 2:176–185.
Mikami A, Ito S, Kubota K. 1982. Visual response properties of dorsolateral prefrontal neurons during visual fixation task. J Neurophysiol. 47:593–605.
Miller EK, Erickson CA, Desimone R. 1996. Neural mechanisms of visual working memory in prefrontal cortex of the macaque. J Neurosci. 16:5154–5167.
Mushiake H, Saito N, Sakamoto K, Itoyama Y, Tanji J. 2006. Activity in the lateral prefrontal cortex reflects multiple steps of future events in action plans. Neuron. 50:631–641.
Narayanan NS, Laubach M. 2006. Top-down control of motor cortex ensembles by dorsomedial prefrontal cortex. Neuron. 52:921–931.
Nelson JI, Salin PA, Munk MH, Arzi M, Bullier J. 1992. Spatial and temporal coherence in cortico-cortical connections: a cross-correlation study in areas 17 and 18 in the cat. Vis Neurosci. 9:21–37.
Nicolelis MAL, Fanselow EE, Ghazanfar AA. 1997. Hebb's dream: the resurgence of cell assemblies. Neuron. 19:219–221.
Nowak LG, Munk MH, James AC, Girard P, Bullier J. 1999. Cross-correlation study of the temporal interactions between areas V1 and V2 of the macaque monkey. J Neurophysiol. 81:1057–1074.
Nowak LG, Munk MH, Nelson JI, James AC, Bullier J. 1995. Structural basis of cortical synchronization. I. Three types of interhemispheric coupling. J Neurophysiol. 74:2379–2400.
O'Reilly RC. 2006. Biologically based computational models of high-level cognition. Science. 314:91–94.
O'Reilly RC, Frank MJ. 2006. Making working memory work: a computational model of learning in the prefrontal cortex and basal ganglia. Neural Comput. 18:283–328.
Owen AM, Doyon J, Petrides M, Evans AC. 1996. Planning and spatial working memory: a positron emission tomography study in humans. Eur J Neurosci. 8:353–364.
Owen AM, Herrod NJ, Menon DK, Clark JC, Downey SP, Carpenter TA, Minhas PS, Turkheimer FE, Williams EJ, Robbins TW, et al. 1999. Redefining the functional organization of working memory processes within human lateral prefrontal cortex. Eur J Neurosci. 11:567–574.
Owen AM, McMillan KM, Laird AR, Bullmore E. 2005. N-back working memory paradigm: A meta-analysis of normative functional neuroimaging studies. Hum Brain Mapp. 25:46–59.
Owen AM, Roberts AC, Hodges JR, Summers BA, Polkey CE, Robbins TW. 1993. Contrasting mechanisms of impaired attentional set-shifting in patients with frontal lobe damage or Parkinson's disease. Brain. 116:1159–1175.
Palm G, Aertsen AM, Gerstein GL. 1988. On the significance of correlations among neuronal spike trains. Biol Cybern. 59:1–11.
Passingham RE. 1972. Non-reversal shifts after selective prefrontal ablations in monkeys (*Macaca mulatta*). Neuropsychologia. 10:41–46.
Passingham RE. 1985. Memory of monkeys (*Macaca mulatta*) with lesions in prefrontal cortex. Behav Neurosci. 99:3–21.
Paz R, Bauer EP, Paré D. 2007. Learning-related facilitation of rhinal interactions by medial prefrontal inputs. J Neurosci. 27:6542–6551.
Perkel DH, Gerstein GL, Moore GP. 1967. Neuronal spike trains and stochastic point processes: II. Simultaneous spike trains. Biophys J. 7:419–440.
Postle BR, Berger JS, D'Esposito M. 1999. Functional neuroanatomical double dissociation of mnemonic and executive control processes contributing to working memory performance. Proc Natl Acad Sci USA. 96:12959–12964.

Rainer G, Asaad WF, Miller EK. 1998. Memory fields of neurons in the primate prefrontal cortex. Proc Natl Acad Sci USA. 95:15008–15013.
Rainer G, Rao SC, Miller EK. 1999. Prospective coding for objects in primate prefrontal cortex. J Neurosci. 19:5493–5505.
Rao SG, Williams GV, Goldman-Rakic PS. 1999. Isodirectional tuning of adjacent interneurons and pyramidal cells during working memory: evidence for microcolumnar organization in PFC. J Neurophysiol. 81:1903–1916.
Riehle A, Grün S, Diesmann M, Aertsen A. 1997. Spike synchronization and rate modulation differentially involved in motor cortical function. Science. 278:1950–1953.
Romo R, Brody CD, Hernandez A, Lemus L. 1999. Neuronal correlates of parametric working memory in the prefrontal cortex. Nature. 399:470–473.
Rougier NP, Noelle DC, Braver TS, Cohen JD, O'Reilly RC. 2005. Prefrontal cortex and flexible cognitive control: rules without symbols. Proc Natl Acad Sci USA. 102:7338–7343.
Rowe JB, Passingham RE. 2001. Working memory for location and time: activity in prefrontal area 46 relates to selection rather than maintenance in memory. Neuroimage. 14:77–86.
Rowe JB, Toni I, Josephs O, Frackowiak RS, Passingham RE. 2000. The prefrontal cortex: response selection or maintenance within working memory? Science. 288:1656–1660.
Saito N, Mushiake H, Sakamoto K, Itoyama Y, Tanji J. 2005. Representation of immediate and final behavioral goals in the monkey prefrontal cortex during an instructed delay period. Cereb Cortex. 15:1535–1546.
Sakurai Y. 1999. How do cell assemblies encode information in the brain? Neurosci Biobehav Rev. 23:785–796.
Sakurai Y, Takahashi S. 2006. Dynamic synchrony of firing in the monkey prefrontal cortex during working-memory tasks. J Neurosci. 26:10141–10153.
Sillito AM, Jones HE, Gerstein GL, West DC. 1994. Feature-linked synchronization of thalamic relay cell firing induced by feedback from the visual cortex. Nature. 369:479–482.
Suzuki H, Azuma M. 1983. Topographic studies on visual neurons in the dorsolateral prefrontal cortex of the monkey. Exp Brain Res. 53:47–58.
Tsujimoto S, Sawaguchi T. 2005. Context-dependent representation of response-outcome in monkey prefrontal neurons. Cereb Cortex. 15:888–898.
Vaadia E, Haalman I, Abeles M, Bergman H, Prut Y, Slovin H, Aertsen A. 1995. Dynamics of neuronal interactions in monkey cortex in relation to behavioural events. Nature. 373:515–518.
Wang XJ. 2001. Synaptic reverberation underlying mnemonic persistent activity. Trends Neurosci. 24:455–463.
Wise SP, Murray EA. 1999. Role of the hippocampal system in conditional motor learning: mapping antecedents to action. Hippocampus. 9:101–117.
Wise SP, Murray EA, Gerfen CR. 1996. The frontal cortex–basal ganglia system in primates. Crit Rev Neurobiol. 10:317–356.
Zaksas D, Pasternak T. 2006. Directional signals in the prefrontal cortex and in area MT during a working memory for visual motion task. J Neurosci. 26:11726–11742.